Middleman, S., *The Flow of High Polymers*, John Wiley & Sons, Inc., New York, 245 (1968).
Pruppacher, H. R., and R. L. Pitter, "A semi-empirical determination of the shape of cloud and rain drops," *J. Atmos. Sci.*, **28**, 86 (1971).
Reynolds, O., "An experimental investigation of the circumstances which determine whether the motion of water shall be direct or sinuous and of the law of resisance in parallel channels," *Trans. Royal Soc. of London*, **A174**, 935 (1883).
Rybczinski, W., Referred to in H. Lamb's *Hydrodynamics*, 1932, Cambridge University Press, 738.
Savic, P., "Circulation and distortion of liquid drops falling through a viscous medium," Nat'l Research Council, Canada Report NRC-MT-22, 50 (1953).
Stokes, G. G., "On the effect of the internal friction of fluids on the motion of pendulums," *Cambridge Phil. Trans.*, **9** (1851).

Manuscript received November 30, 1981; revision received May 3, and accepted May 28, 1982.

Plasma—Particle Momentum and Heat Transfer: Modelling and Measurements

Measurements were made of the two-dimensional flow and temperature field in a d.c. plasma jet under different operating conditions. The particle velocity and the in-flight particle temperature were also measured for narrow cuts of alumina powders, of mean particle diameters of 18, 23, 39 and 46 μm, injected in the jet. The results are compared with the predictions of a one-dimensional mathematical model. The measured and computed particle velocities are in good agreement. This is, however, not the case for the particle temperature where considerable differences are observed. An attempt is made to determine the parameters which are often unduly neglected in modelling work and to identify the areas where further work is needed.

M. VARDELLE, A. VARDELLE, P. FAUCHAIS
Université de Limoges, France
and
M. I. BOULOS
Université de Sherbrooke
Québec, Canada

SCOPE

One of the applications of thermal plasma technology that has gained a wide acceptance on an industrial scale is plasma spray-coating. Presently, plasma spray-coating is used in a number of areas of the aerospace and manufacturing industries for the deposition of refractory and erosion-resistant coatings. Other applications such as wear resistance and weather-protection coatings are getting increasing attention. In either case, the basic technique used involves the injection of the powdered coating material in the tail flame of a d.c. plasma jet. As the particles are entrained by the jet, they are accelerated to a relatively high velocity, heated up and molten in a very short time. The formed droplets are then projected towards the substrate to be coated. On impact, the droplets solidify almost instantly and adhere to the surface of the substrate.

The quality of the coating is found to depend to a large extend on the particle velocity prior to the impact and whether or not all the particles were completely molten. Improvement of the quality of the coating obtained necessitated an intense research effort directed towards the study of the flow and temperature fields in a d.c. plasma jet and the characterization of the particle trajectory, temperature history and gas-particle heat transfer under plasma conditions. A special attention has also been given to the mathematical modelling of such a relatively complex system.

This paper reports an experimental and theoretical study of the gas and particle dynamics under conditions typically used in plasma spray-coating. The work involved the measurement of the gas velocity and temperature in d.c. plasma jet under different operating conditions. Measurements were also made of particle velocity and in-flight particle temperature for alumina particles injected in the jet. The results are compared with the predictions of a mathematical model.

CONCLUSIONS AND SIGNIFICANCE

From a comparison of the obtained experimental measurements and the predictions of a relatively simple one-dimensional mathematical model, it can be seen that the proposed model is adequate for the calculation of the particle velocity in the jet. The model, however, is far from being satisfactory when it comes to the calculation of the temperature history of the particles. In fact, contrary to experimental evidence, the model gave rise to very fast heating-up rates and melting of the particles. The difference could be due to the fact that resistance to internal heat transfer in the particles was neglected. It also could result from other effects not accounted for in the model such as thermophorises or carrier gas cooling, which could influence the particle trajectory and prevent it from penetrating the hot core of the jet.

The principal contribution of this work lies in the fact that it is the first time a comprehensive set of measurements is reported of the plasma velocity and temperature fields as well as the particle velocity and its in-flight temperature. From a comparison of this data with the predictions of the mathematical model, an attempt is made to determine the parameters which were unduly neglected in the model and to identify the areas where further work is needed.

0001-1541-83-6722-0236-$2.00.

INTRODUCTION

Over the last few years, a number of mathematical models have been developed for the calculation of the trajectories and temperature histories of particles as they are injected in a plasma torch. These varied from relatively simple one-dimensional models such as those proposed by Yoshida (1977) and Gal-Or (1980) to more elaborate two-dimensional models proposed by Boulos and Gauvin (1974), Boulos (1978), Bhattacharyya and Gauvin (1975), Fiszdon and Lesinski (1975), and Fiszdon (1979).

While most of these models were developed for the thermal treatment of powders in a d.c. plasma torch, a few were applied to the induction plasma (Yoshida, 1977; Boulos, 1978). In either case, the models varied in the assumptions made and whether or not they took into account the effects of internal heat conduction in particles on the overall heat transfer process between the plasma and the particles. Only Yoshida (1977) and Fiszdon (1979) considered the internal heat conduction in the particles, while the others assumed the particles to have a uniform temperature.

It may be noted, however, that while much effort has been devoted to the modelling work, little attention has been given to the experimental verification and the validation of the model predictions. This is largely attributed to experimental difficulties encountered in the measurement of the in-flight particle parameters such as its velocity, temperature, diameter and composition.

The objectives of the present study was specifically to obtain sufficient experimental information on the particle parameters during its flight in a d.c. plasma jet and to compare the results with the prediction of a relatively simple one-dimensional model in order to evaluate its capabilities and identify the areas where further work is needed. The task was by no means an easy one since some of the experimental techniques used such as laser doppler anemometry and in-flight particle temperature measurements are still the subject of considerable development work.

In this paper, only a brief outline will be given of the experimental techniques. Emphasis will be made on the comparison of the experimental data with the model predictions. A detailed account of the experimental set-up and data analysis can be found elsewhere (A. Vardelle, 1979; M. Vardelle, 1980; Vardelle et al., 1980).

EXPERIMENTAL TECHNIQUES

The study was carried out on a d.c. plasma torch of a standard design. Details of the geometry of the anode nozzle and the system of coordinates are given in Fig. 1. The torch was operated using either a mixture of nitrogen-hydrogen or argon-hydrogen as the plasma gas which necessitated the use of anodes of different internal diameters. The dimensions of the anodes used are given in Table 1 together with the corresponding gas flow rates, torch current, voltage drop, power, and energy efficiency.

The powder injected in the plasma was a narrow cut of pure alumina. The powder characteristics and the corresponding radial injection velocity, v_{pi}, are given in Table 2. In each case, the injection velocity was chosen in a way to insure a maximum velocity of the particles along the centerline of the torch. It also gave rise to good penetration and a uniform distribution of the particles in the plasma jet.

In order to achieve a comprehensive validation of the mathematical model, the following measurements were carried out on the same d.c. torch under identical experimental conditions:

- Plasma temperature field
- Plasma velocity field
- Particle velocity distribution
- Particle temperature distribution

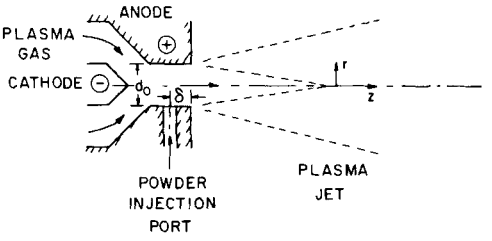

Figure 1. Torch geometry and system of coordinates.

TABLE 2. POWDER CHARACTERISTICS AND THEIR CORRESPONDING INJECTION VELOCITY

Powder	$\overline{dp}$ μm	σ_g	v_{Pi} (N_2/H_2 Plasma) m/s	v_{Pi} (Ar/H_2 Plasma) m/s
A	18	1.18	25.0	32.0
B	23	1.19	22.0	29.0
C	39	1.20	18.0	24.0
D	46	1.20	14.0	19.0

Plasma Temperature Field Measurements

Since a d.c. plasma jet, temperatures of 10,000–12,000 K can be encountered, conventional temperature measurement techniques are not satisfactory and it is necessary to use more specialized techniques such as atomic or molecules spectral line emission. (Fauchais et al., 1979). Atomic emission spectroscopy has the advantage of high spacial resolution but is limited to temperatures above 6,000 K. Below 2,000 K, temperatures were measured using chromel-alumel thermocouples. Only a few points could be obtained in the range 2,000–6,000 K corresponding to the melting point of refractory materials such as pure alumina and tungsten (2,326 K for Al_2O_3 and 3,680 K for W). Both the thermocouple and m.p. temperature measurements were corrected for conduction along the stem of the probe and for radiation losses.

The experimental set-up used for the spectroscopic temperature measurements consisted essentially of a J.Y THR 1500 monochromator equipped with a holographic grating with 3,200 lines/mm and a dispersion of 1.1 nm/mm. The measurements were carried out using the absolute intensity of the NI 7,468 Å line. The system was calibrated using a standard tungsten ribbon lamp.

Plasma and Particle Velocity Measurements

The plasma and particles velocities were determined using laser doppler anemometry. A schematic of the experimental set-up is shown in Figure 2. Both the fringe and the two-point measurement systems were used. The former was used for the measurement of the particle velocities as they are entrained in the jet, while the later was used to measure the plasma velocity or, more precisely, the velocity of fine alumina tracer particles ($\overline{d}_p = 3 \pm 1.5\ \mu$m) which were dispersed in the flow. These were estimated to be fine enough to give a good measure of the time averaged gas velocity (Richards, 1977) while not evaporating during their short residence time in the flow.

In the fringe measurement system, Figure 2a, a 1.2 W Argon ion laser beam (λ = 514.5 nm) was split into two beams which were then focused to form an interference fringe pattern in the flow region. As a particle passed through the point of intersection of these two beams, it produced a light burst with a modulation frequency function of its velocity component perpendicular to the fringe pattern and the fringe spacing.

The scattered light was collected by a lens and concentrated on the entrance slit of a photomultiplier. The electrical signal delivered by the photomultiplier was processed by photon correlation techniques to deter-

TABLE 1. NOZZLE DIMENSIONS AND TORCH OPERATING CONDITIONS

Nozzle Dimensions* d_o, frmm	δ, mm	Gas Flow Rates L/min	Current A	Voltage V	Power kW	Efficiency %
6.0	2.0	37 L/min N_2 + 11 L/min H_2	290	100	29.0	72.0
8.0	2.0	75 L/min Ar + 15 L/min H_2	290	100	29.0	63.0

* See Figure 1 for legend.

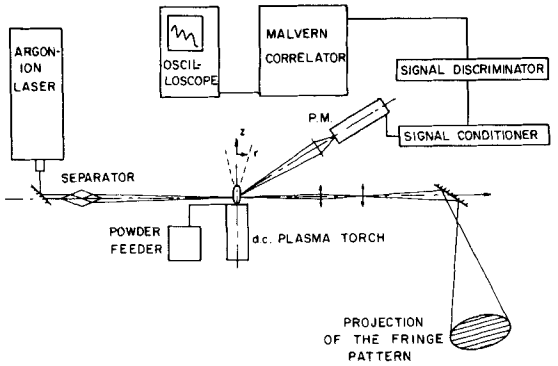

Figure 2a. Schematic of the laser doppler anemometer set-up, the fringe system.

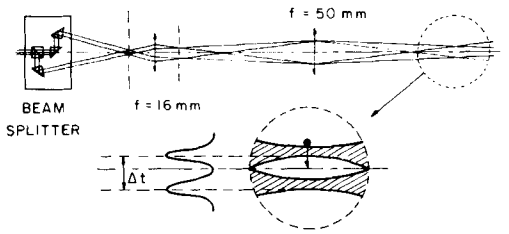

Figure 2b. Laser beam arrangement used for the two-point laser anemometry measurements.

mine the average modulation frequency, and thus the average particle velocity. The axial and radial velocity components of the particles could be obtained simply by rotating the fringe pattern around its axis.

Because of the relatively high power of the laser beam, observations could be made of the light scattered by the particles at 90° to the laser axis. The measuring volume was in the form of a cylinder 600 μm in diameter and 1.1 mm long. The fringe spacing was 100 μm.

In the two-point measurement system the laser beam after passing through a beam splitter was focussed using a microscopic lense to form two coherent thin light beams each 50 μm diameter, 400 μm apart. The two beams were projected in the plasma jet by a lens with a magnification of unity. Details of the laser beam arrangement in this case are given in Figure 2b.

Each beam focus was further imaged onto the entrance slit of two photomultipliers equipped with a narrow band interference filter (λ = 514.5 nm and $\Delta\lambda$ = 0.25 nm). The output of the two photomultipliers were cross-correlated by the photon correlator. As a particle crossed the two beams in the measuring volume, it produced two successive light bursts, the time delay between them was function of the particle velocity and the distance between the two beams.

In-Flight, Particle Surface Temperature Measurements

The in-flight particle surface temperature measurements were by far the most demanding of the diagnostic techniques used. They were made, following a method proposed by Kruszewska and Lesinski (1977), in which the particle temperature is determined by an analysis of the radiation emitted from its surface. A schematic of the experimental set-up used is shown in Figure 3.

An image of the plasma jet is focused into the entrance slit of a cooled photomultiplier (RCA C 31 034C) sensitive in the near infrared over the spectral range between 850 and 1,050 nm. The amplitude of the current pulses generated by the passage of each particle across the measuring volume is function of the particle diameter, its shape, surface emissivity and temperature. Using narrow size cuts of spherical alumina particles for which the surface emissivity are known in the solid and liquid states, it was possible to estimate the surface temperature of the particle from the height of the PM signal. In order to limit our measuring volume to a parallelopiped 100 × 100 μm by 200 μm long, a second photomultiplier (PM-2 in Figure 3) was used for coincidence analysis. This was an RCA 1 P 28 sensitive over the spectral range from 200 to 700 nm. A yellow filter placed in front of the entrance slit of the PM protected it from the background plasma radiation. Calibration was carried out using a tungsten ribbon lamp placed behind a chopper containing a small aperture and rotating at a constant speed (Figure 3).

It is important to point out that uncertainties in the values of the surface

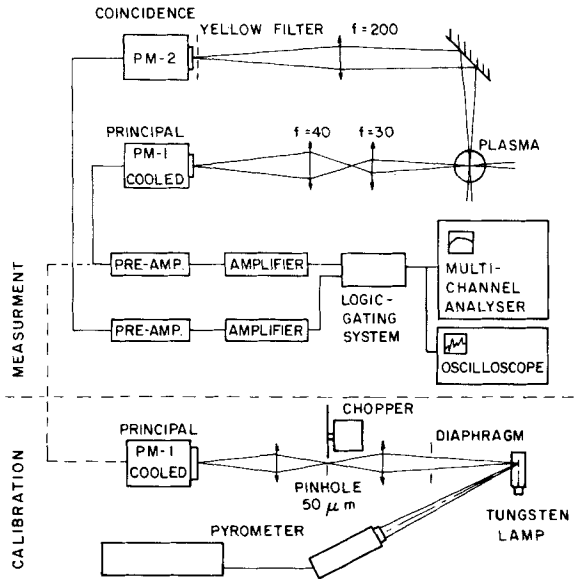

Figure 3. Schematic of the experimental set-up used for the in-flight particle surface temperature measurements.

emissivities used (ϵ = 0.5 for solid alumina and 0.9 for the molten alumina) could introduce an accuracy error of about 10 to 15% in the temperature measurements. The precision error, however, was estimated to be less than 5%.

RESULTS AND DISCUSSION

Plasma Temperature and Flow Fields

Typical results obtained with the N_2/H_2 plasma at a power level of 29 kW are given on Figures 4–6.

Figure 4a gives the temperature isocontours in the jet. Three distinct regions are noted. The core region in which the plasma temperature is relatively constant, 12,000–12,500 K, extends to about 10 to 12 mm from torch nozzle. This is followed by a transition region in which the plasma temperature falls very rapidly to less than 3,000 K at 100 mm from the nozzle. Finally there is the fully developed region in which the gas temperature drops rather gradually as it is fully mixed with the entrained ambient air. The radial temperature profiles are particularly steep over the core region. As shown in Figure 5, a temperature drop of more than 4,000 K has been measured over a distance of 1 mm. It is specifically the presence of such steep temperature gradients that makes the problem of the thermal treatment of particles in a d.c. plasma jet difficult and necessitates a close control on the particle-size distribution and injection conditions in the plasma jet.

Figure 4b gives the axial velocity isocontours. As mentioned earlier, these were obtained by seeding the flow with fine alumina

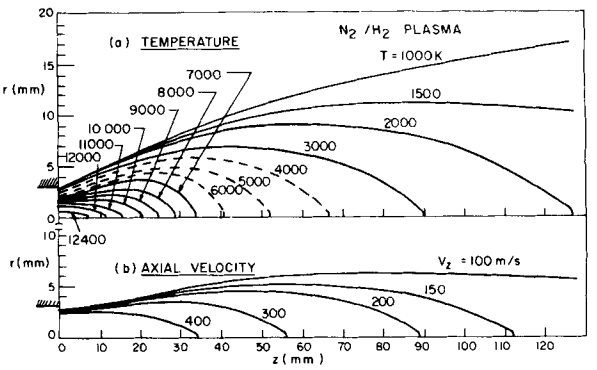

Figure 4. Temperature and axial velocity isocontours for the nitrogen/hydrogen plasma.

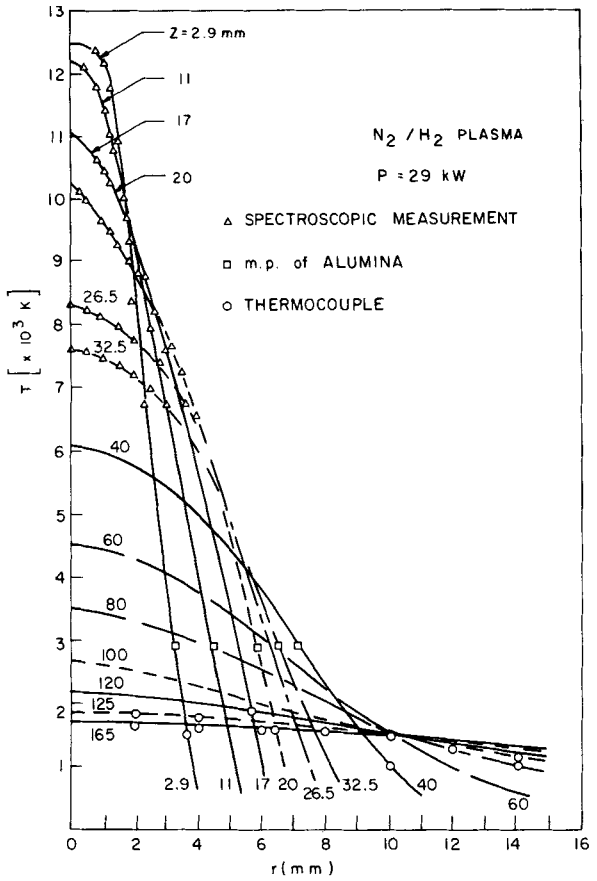

Figure 5. Radial temperature profiles for the nitrogen/hydrogen plasma.

dispersed in the plasma upstream of the nozzle. It was, however, rather difficult to obtain a uniform seeding in the core of the jet ($r < 2$ mm and $z < 10$ mm); thus, no significant plasma velocity measurements could be made in this region of the flow.

Beyond the core region, the plasma velocity dropped rapidly with the increase of the distance from the nozzle. As was the case for the radial temperature profiles, the plasma axial velocity dropped also rapidly with the radial distance from the axis of the torch. This is particularly evident at $z = 5$ mm and $r = 2$ mm where

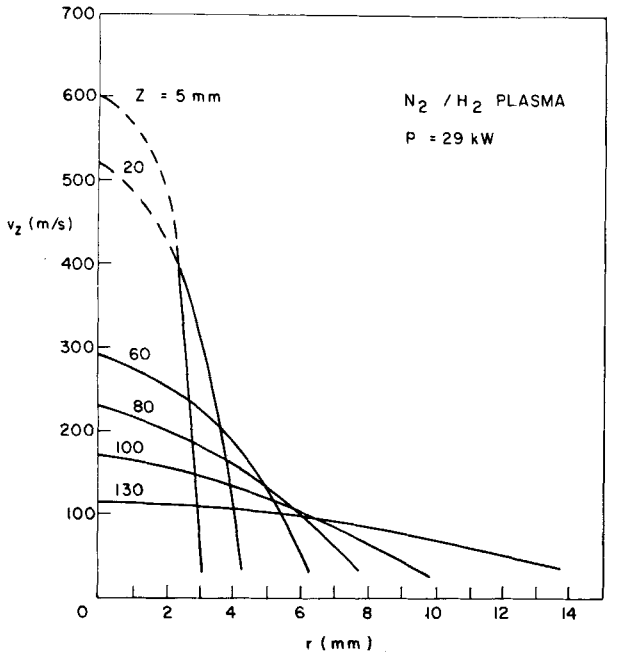

Figure 6. Axial velocity profiles for the nitrogen/hydrogen plasma.

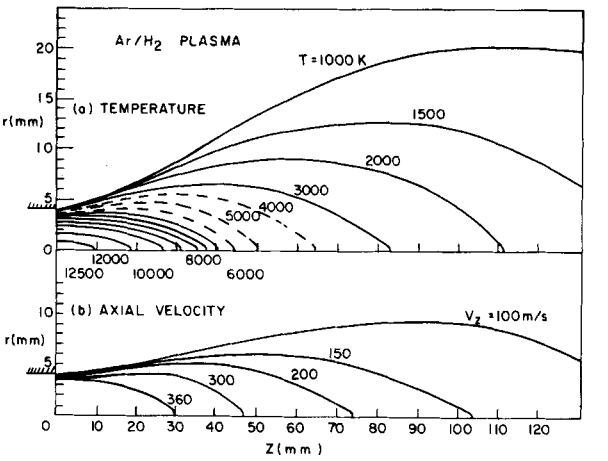

Figure 7. Temperature and axial velocity isocontours for the argon/hydrogen plasma.

the plasma velocity drops from about 400 m/s to less than 50 m/s in a distance of about 1 mm in the radial direction.

Similar results were obtained with an Ar/H_2 plasma under essentially the same operating conditions (Figures 7 to 9). It should be pointed out that in this case the total plasma gas flow rate and composition has been adjusted in such a way to keep the total power dissipated in the torch constant (29 kW). The total gas flow rate in this case was equal to 90 L/min with a hydrogen concentration of 16.7% by volume, compared to 48 L/min and 23% by volume for the N_2/H_2 plasma.

It is noticed that the core region of the jet in this case is longer and narrower than that for the N_2/H_2 plasma. The jet, however, spreads faster further downstream compared to the N_2/H_2 case. Figure 8 shows that the temperature level in the core region is still in the range of 10,000–12,500 K with the presence of very steep temperature gradients at the edges of the core region.

The axial velocity profiles for the Ar/H_2 plasma given in Figure

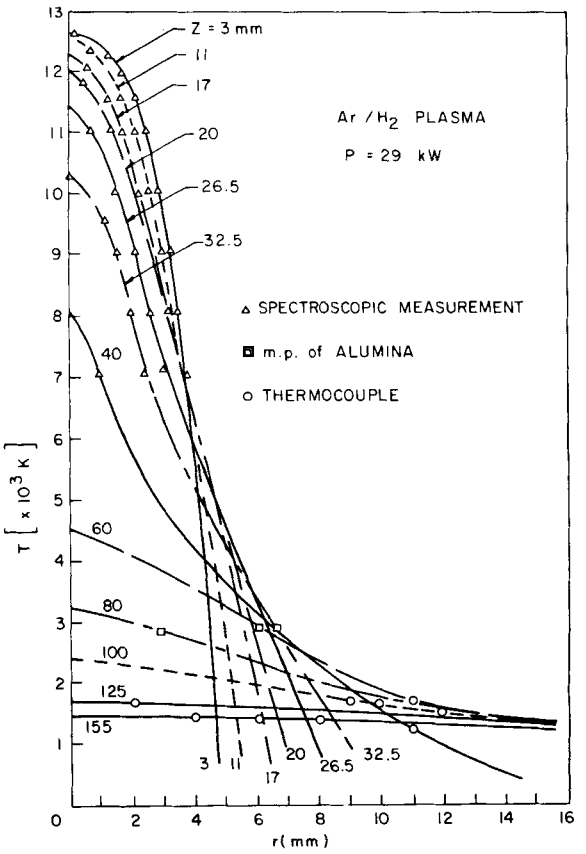

Figure 8. Radial temperature profiles for the argon/hydrogen plasma.

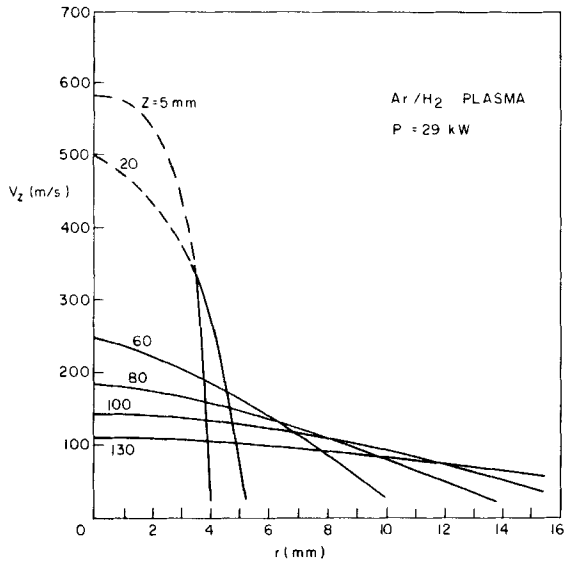

Figure 9. Axial velocity profiles for the argon/hydrogen plasma.

9 shows essentially the same features as that for the N_2/H_2 plasma with the velocity at the edge of the core region reaching as high as 300–400 m/s. Here again it was not possible, due to seeding difficulties, to obtain precise plasma velocity measurements in the core of the jet.

Particle Velocity Measurements

Measurements were made of the axial velocity profiles of different narrow cuts of pure alumina particles injected in the N_2/H_2 and the Ar/H_2 plasmas under essentially the same operating conditions.

Typical results for powder A ($\bar{d}_p = 18\ \mu m$, $\sigma_g = 1.18$) injected at a mean radial velocity of 25 m/s in a N_2/H_2 plasma jet are given in Figure 10. It is noticed that the particle accelerates rapidly, as it is entrained by the plasma and reaches a maximum velocity of 275 m/s on the axis of the torch, 60 mm from the nozzle. Further downstream the axial particle velocity drops gradually attaining

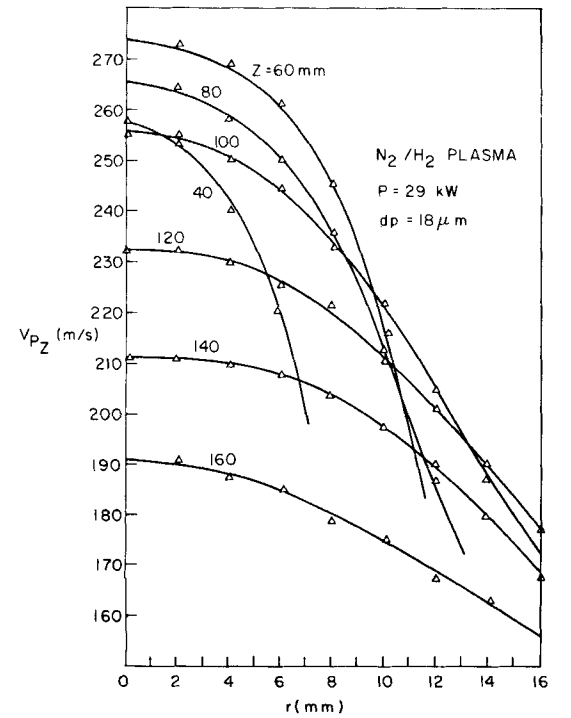

Figure 10. Particle axial velocity profiles for the N_2/H_2 plasma.

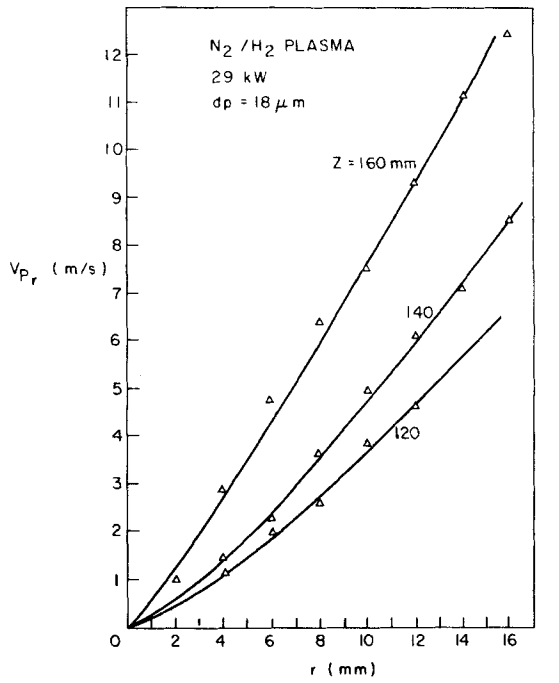

Figure 11. Particle radial velocity profiles for the N_2/H_2 plasma.

190 m/s at 160 mm. They also spread in the jet within ± 16 mm from the axis of the flow. The radial velocity of the particles is considerably lower than the axial velocity as shown in Figure 11. This is particularly important since it supports the simplifying assumption made in the development of the mathematical model that the particles have essentially an axial trajectory.

The variation of the axial velocity profiles along the centerline of the torch for different powders is given on Figure 12. As expected the smaller particles, because of their lower inertia, are accelerated much faster by the flow compared to the heavier particles. The latter, however, once they attain their maximum velocity at a distance of about 60 to 80 mm from the nozzle, maintain their momentum and eventually move at a higher velocity than that of the gas at a distance of 140 to 160 mm from the nozzle.

Similar results were also obtained for the Ar/H_2 plasma as shown in Figures 13 and 14, although the maximum velocity attained by

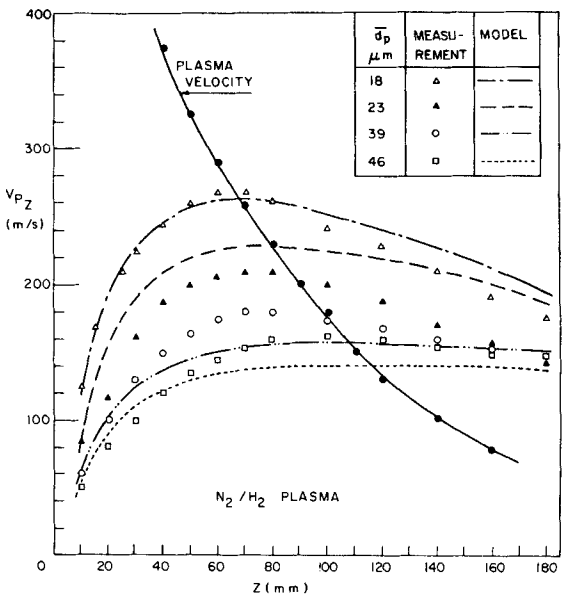

Figure 12. Particle axial velocity along the centerline of the N_2/H_2 plasma jet, P = 29 kW.

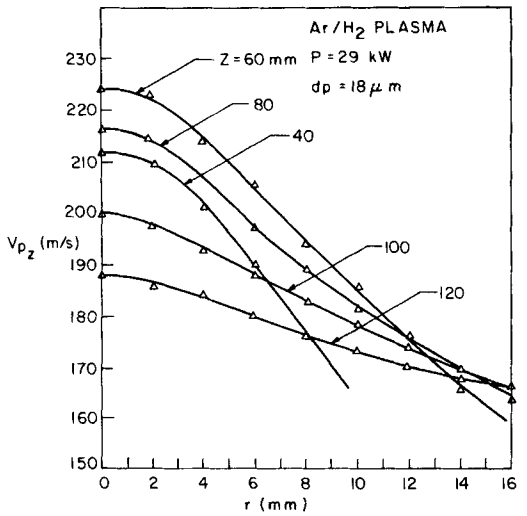

Figure 13. Particle axial velocity profiles for the Ar/H_2 plasma.

the particles in this case was lower than that obtained for the N_2/H_2 plasma (275 m/s for an 18-μm particle in a N_2/H_2 plasma compared to 220 m/s for the same particle in an Ar/H_2 plasma). The effect, however, is hardly noticed for the heavier particles, since from a comparison of the results on Figures 12 and 14, a 46 μm particle attains essentially the same maximum velocity of 140 m/s at about 100 mm from the nozzle independent of the plasma gas used (N_2/H_2 or Ar/H_2).

Particle Temperature Measurements

Relatively few data points could be obtained for the in-flight particle temperature due to numerous experimental difficulties encountered. Typical results obtained with the 18-μm particles (powder A) with the N_2/H_2 plasmas are given in Figure 15. It is noticed that the particle surface temperature reaches the melting point of alumina of 2,326 K in less than 30 mm from the point of injection. The particles, however, seems to remain at that temperature for quite a long time during their flight along the axis of the plasma until they eventually start to cool down and solidify at about 120 mm from the nozzle. As expected, the point at which the particle surface temperature starts to drop coincides with the point at which the plasma temperature drops below that of the particle.

MATHEMATICAL MODEL

In order to calculate the particle trajectories and temperature histories as they are injected in the plasma jet, a simplified one-dimensional mathematical model was developed based on the following assumptions.

1. One-dimensional flow in which the particles maintain an axial trajectory along the centerline of the jet.
2. Spherical particles with negligible internal temperature gradients.
3. Low particle loading ratio in the plasma. This implies that there is no particle-plasma interaction.
4. The plasma is in local thermodynamic equilibrium and is optically thin.
5. Negligible gravitational effects.

GOVERNING EQUATIONS

Based on the above assumptions the equations governing the momentum and heat transfer between the particles and the plasma can be written as follow.

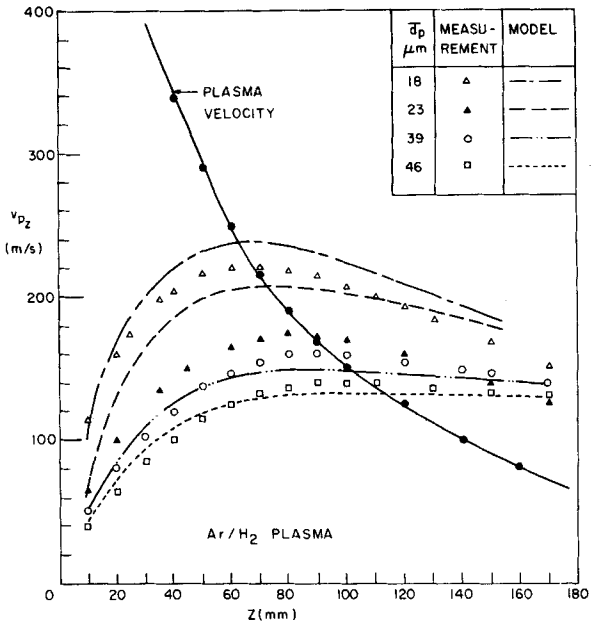

Figure 14. Particle axial velocity along the centerline of the Ar/H_2 plasma jet, P = 29 kW.

Particle Velocity

$$\frac{dU_{Pz}}{dt} = \frac{3}{4} C_D (U_{Pz} - U_f)|U_{Pz} - U_f|(\rho_f/\rho_p d_p) \qquad (1)$$

where C_D is the drag coefficient given by the following correlations as function of the Reynolds number ($Re = \bar{\rho}_f|U_{Pz} - U_f|d_p/\bar{\mu}_f$).

$$C_D = 24/Re \qquad \text{for } Re < 0.2 \qquad (2)$$

$$C_D = (24/Re)[1 + 0.187\,Re] \qquad 0.2 \le Re < 2.0 \qquad (3)$$

$$C_D = (24/Re)[1 + 0.110\,Re^{0.81}] \qquad 2.0 \le Re < 21.0 \qquad (4)$$

$$C_D = (24/Re)[1 + 0.189\,Re^{0.62}] \qquad 21.0 \le Re < 500 \qquad (5)$$

Equation 2 is based on the Stokes solution for the flow around a sphere and Eq. 3 is based on the Oseen approximation (Schlichting, 1968). Equations 4 and 5 are based on the experimental data by Beard and Pruppacher (1969) which were confirmed by the numerical computations of Hamielec, Hoffman and Ross (1967).

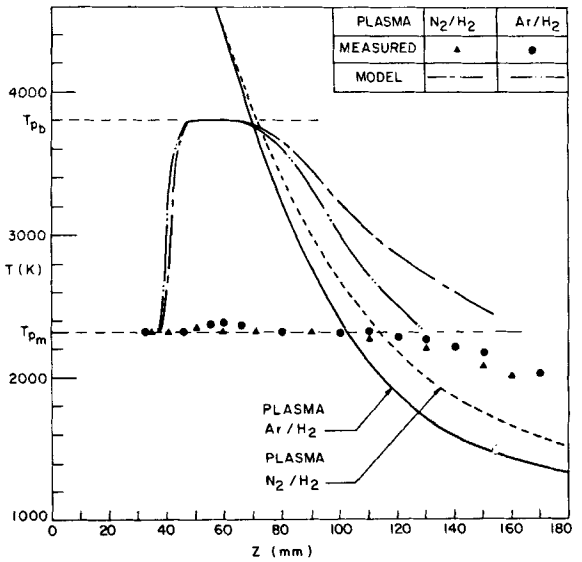

Figure 15. Particle temperature profiles along the centerline of the plasma jet for the N_2/H_2 and Ar/H_2 plasmas, 29 kW, $\bar{d}_p$ = 18 μm.

TABLE 3. THERMODYNAMIC PROPERTIES OF PURE ALUMINA

Density	$\rho_p = 3.9 \times 10^3$ kg/m^3
Melting Point	$T_m = 2{,}326$ K
Boiling Point	$T_b = 3{,}800$ K
Latent Heat of Fusion	$\lambda_m = 1.065 \times 10^6$ J/kg
Latent Heat of Vaporization	$\lambda_v = 2.467 \times 10^7$ J/kg
Emissivity	$\epsilon = 0.3$ for $T < 2{,}326$ K
	$\epsilon = 0.9$ for $T > 2{,}326$ K

Specific Heat; J/kg·°C

$C_p = 27.43 + 3.06 \times 10^{-3}\, T - 8.47 \times 10^5/T^2$ for $T \leq 1{,}273$ K

$C_p = 25.48 + 4.25 \times 10^{-3}\, T - 6.28 \times 10^5/T^2$ for $T \leq 2{,}316$ K

$C_p = 34.62$ for $2{,}326 < T$ K

Particle Temperature

The particle temperature was determined by an energy balance giving rise to the following equation.

$$\frac{dT_p}{dt} = \frac{Q}{mc_p} \tag{6}$$

where Q is the net heat transfer rate to the particle

$$Q = a_p h(T_f - T_p) - a_p \epsilon \sigma (T_p^4 - T_a^4) \tag{7}$$

where the 1st term on the RHS of Eq. 7 represents the conductive and convective heat transfer between the particle and the plasma while the second term represents the heat lost by radiation from the surface of the particle to its surroundings ($T_a = 300$ K).

The heat transfer coefficient was estimated using the Ranz and Marshall equation (Ranz and Marshall, 1952)

$$Nu = 2.0 + 0.514\, Re^{0.5} \tag{8}$$

Special attention was given to the effect of steep temperature gradients on the variation of the property values of the plasma across the boundary layer of the particles. These were evaluated by taking the integral mean of the property between the particle surface temperature and the temperature of the plasma calculated as follows:

$$\bar{k}_f = \frac{1}{(T_f - T_p)} \int_{T_p}^{T_f} k\, dT \tag{9}$$

A similar equation was used to evaluate $\bar{\mu}_f$ and $\bar{\rho}_f$, respectively. As the particle temperature reached its melting point, its temperature was assumed to remain constant and the rate of change of the fraction of the particle molten, x, was calculated using Eq. 10.

$$\frac{dx}{dt} = \frac{Q}{m\lambda_m} \tag{10}$$

where λ_m is the latent heat of fusion of the particle. The same equation was also applied to the solidification of a liquid dropplet during its cooling period as it emerged from the plasma.

Once the particle was completely molten, $x = 1.0$, its temperature was allowed to rise again governed by Eq. 6 until it eventually reached its boiling point where it would start to evaporate. The particle temperature was then maintained constant and its diameter allowed to decrease according to Eq. 11.

$$\frac{dd_p}{dt} = \frac{-2Q}{\rho_p \lambda_v \Pi d_p^2} \tag{11}$$

where λ_v is the latent heat of vaporization of the particle.

MODEL PREDICTIONS VS. EXPERIMENTAL DATA

Computations were carried out for pure alumina particles under the same conditions as that used in the experimental measurements. The physical properties of the alumina are summarized in Table 3. The particles were assumed to be initially on the centerline of the plasma jet at a distance of 10 mm from the nozzle. Their initial temperature and axial velocity were assumed to be that measured experimentally at the same point.

The computed particle velocity along the centerline of the jet for different particle sizes are superimposed on Figures 12 and 14 for comparison. It is interesting to note a relatively good agreement between the model predictions and the experimental values for the 18-μm particles. The agreement, however, is less satisfactory for the 23-μm particles where a noticeable deviation appears further downstream at $z = 160$ mm. This could be related to the uncertainty in the plasma velocity measurements in the core region which were particularly difficult due to the plasma seeding problems. It could also be a result of the uncertainty in the trajectory and temperature history of the particles from their point of injection in the side of the nozzle until they reached the centerline of the jet.

Obviously a substantial improvement in the model predictions can be achieved by a closer investigation of the flow and temperature fields near the point of injection of the powder. Specifically it would be important to examine the influence of the powder carrier gas on the overall particle trajectory and temperature history. The flow in this region, however, is quite complex and has a distinct three-dimensional character. Thermophorises is also another parameter which has not been taken into account by the present model and could influence the initial particle trajectory. It should be pointed out, however, that since there has been no detailed study of thermophorises under plasma conditions, all attempts to estimate the magnitude of the thermophoretic force acting on a particle in a plasma jet or an arc column has to use thermophorises coefficients experimentally measured under substantially lower temperature gradients.

A comparison of the computed and the measured particle temperatures along the centerline of the jet is given on Figure 15. Unfortunately in this case the computed particle temperatures are considerably different from the experimental values.

While the difference could be partly attributed to experimental uncertainty in the estimation of the in-flight temperature of the particle, it could also result from the assumption of negligible internal heat gradients in the particle. As shown by Bourdin et al. (1980), an alumina particle 100 μm in diameter, suddenly immerged in a plasma surrounding can build up as much as 1,000 K temperature difference between its surface and center point before reaching its melting point. Moreover, as the particle surface starts to melt, the propagation of the fusion front can have an important retarding effect on the internal heat transfer in the particle and in turn, slow down the melting process. Obviously, any substantial improvement of the model from a heat transfer point of view has to take into account, as a first step, at least for refractory and poor conduction materials, internal heat transfer phenomena in the particles.

CONCLUSION

Measurements have been made of the plasma and particle velocity and temperatures histories in a d.c. plasma jet under different operating conditions. These are compared with the predictions of a one-dimensional mathematical model. While the model predictions are in good agreement with the particle velocity measurements, considerable differences exist between the computed and the measured particle temperatures. Further work is needed to study the flow and temperature fields in the neighborhood of the point of powder injection which can have an important influence on the overall particle trajectory in the plasma. Improvement of the model capabilities will also have to include as a first step internal heat conduction in the particles which can have an important influence on its overall temperature history.

ACKNOWLEDGMENT

This work was partially supported by the French and Quebec governments through a France-Quebec exchange program.

NOTATION

a_p = particle surface area, m^2
C_D = drag coefficient
d_o = nozzle diameter, m
d_p = particle diameter, m
h = heat transfer coefficient, $W/cm^2 \cdot K$
m = particle mass, kg
Nu = Nusselt number, $hd_p/\bar{k}$
Q = net heat flow to the particle, Eq. 7, W
r = distance in the radial direction, mm
Re = Reynolds number $[\bar{\rho}_f|U_{Pz} - U_f|d_p/\bar{\mu}_f]$
t = time, s
T_a = ambient temperature, K
T_f = field temperature
T_p = particle temperature, K
U_f = axial fluid velocity, m/s
U_{Pz} = axial particle velocity, m/s
v_{Pl} = radial particle injection velocity, m/s
x = mass fraction of the particle in the liquid state
z = distance in the axial direction, mm
σ_g = geometric standard deviation of the powder size
ρ_f = fluid density, kg/m^3
ρ_p = particle density, kg/m^3
μ_f = fluid viscosity, kg/m·s
ϵ = particle emissivity
σ = Stefan-Boltzman constant
λ_m = laten heat of fusion, J/kg
λ_v = laten heat of vaporization, J/kg

LITERATURE CITED

Beard, K. V., and H. R. Pruppacher, "A determination of the terminal velocity and drag of small water drops by means of a wind tunnel," *J. Atmos. Sc.*, **26**, 1066 (1969).

Bhattacharyya, D., and W. H. Gauvin, "Modelling of heterogeneous systems in a plasma jet reactor," *AIChE J.*, **21**, 879 (1975).

Boulos, M. I., "Heating of powders in the fire-ball of an induction plasma," *IEEE Trans. on Plasma Sc.*, **4**, 93 (1978).

Boulos, M. I., and W. H. Gauvin, "Powder processing in a plasma jet, a proposed model," *Can. J. Chem. Eng.*, **52**, 355 (1974).

Bourdin, E., P. Fauchais, and M. I. Boulos, "Transient heat conduction to a single sphere under plasma conditions," National Heat Transfer Symposium, Edmonton, Alberta (Oct. 19–22, 1980).

Fauchais, P., K. Lapworth, and J. M. Baronnet, eds., "First report on measurements of temperature and concentration of excited species in optically thin plasmas," IUPAC (1979).

Fiszdon, J. K., "Melting of powder grains in a plasma flame," *Int. J. Heat and Mass Transfer*, **22**, 749 (1979).

Fiszdon, J. K., and J. Lesinski, "Accélération et fusion des grains dans un jet de plasma d'argon-hydrogène," International Round Table on Study and Applications of Transport phenomena in thermal plasmas, Odeillo, France (Sept. 12–16, 1975).

Gal-Or, B., "Plasma-spray coating processes; physico-mathematical characterization," *J. of Eng. for Power*, **102**, 589 (1980).

Hamielec, A. E., T. W. Hoffman, and L. L. Ross, "Numerical solution of the Navir-Stokes equation for flow past spheres," *AIChE J.*, **13**, 212 (1967).

Kruszewska, B., and J. Lesinski, "Temperature distributions of solid particles in a plasma stream," *Rev. de physique Appl.*, **12**, 1203 (1977).

Ranz, W. E., and W. R. Marshall, Jr., "Evaporation from drops," *Chem. Eng. Prog.*, **48**, 141 (1952) and **48**, 173 (1952).

Richards, B., ed., "Measurement of unsteady fluid dynamic phenomena," McGraw Hill (1977).

Schlichting, "Boundary Layer Theory," McGraw Hill, 6th ed. (1968).

Vardelle, A., "Contribution à la mesure statistique des vitesses et des températures de surface de particules injectées dans un jet de plasma d'arc," Thèse de doctorat 3e cycle, Université de Limoges, France (1979).

Vardelle, A., J. M. Baronnet, M. Vardelle, and P. Fauchais, "Measurements of the plasma and condensed particles parameters in a d.c. plasma jet," *IEEE Trans. on Plasma Sc.*, **8**, 417 (1980).

Vardelle, M., "Etude de la structure des dépôts d'alumine obtenus par projection à plasma en fonction des températures et des vitesses des particules au moment de leur impact sur la cible," Thèse doctorat 3e cycle, Université de Limoges, France (1980).

Yoshida, T., and K. Akashi, "Particle heating in a radio-frequency plasma torch," *J. Appl. Phys.*, **48**, 2252 (1977).

Manuscript received October 8, 1981; revision received April 2, and accepted April 26, 1982.

Fault Diagnosis in Nonlinear Chemical Processes

Part I. Theory

We propose a two-level identification strategy to detect and diagnose process faults and their causes. The strategy can be applied to processes represented by process models nonlinear in the states but linear in the coefficients. Relations to calculate both the observer for the states and the least squares estimator for the coefficients are specified in detail.

K. WATANABE and D. M. HIMMELBLAU

Department of Chemical Engineering, The University of Texas, Austin, TX 78712

SCOPE

A two-level strategy for the detection and diagnosis of faults in industrial processes is presented. By fault is meant degradation in process performance; by diagnosis is meant identification of the cause(s) of the fault. Faults can be related quantitatively to elements in process models including both the states and the parameters. Detection of a change and the isolation of the reasons for the change in the process parameters are problems of both theoretical and practical interest in the process industries.

Previous work has focused on the use of simultaneous estimation of the model states and parameters or hierarchical

K. Watanabe is on leave from Hosei University at Koganei, Tokyo, Japan.